

Research Article: New Research | Disorders of the Nervous System

Rapid increases in proBDNF after pilocarpine-induced status epilepticus in mice are associated with reduced proBDNF cleavage machinery

ProBDNF is acutely elevated post-status epilepticus

Ajay X. Thomas^{1,2,3}, Yasmin Cruz Del Angel¹, Marco I. Gonzalez^{1,2}, Andrew J. Carrel^{1,2}, Jessica Carlsen¹, Philip M. Lam¹, Barbara L. Hempstead⁴, Shelley J. Russek⁵ and Amy R. Brooks-Kayal^{1,2,6}

¹Department of Pediatrics, University of Colorado Anschutz Medical Campus, Aurora, CO

²Neuroscience Program, University of Colorado Anschutz Medical Campus, Aurora, CO

³Medical Scientist Training Program, University of Colorado Anschutz Medical Campus, Aurora, CO

⁴Departments of Medicine, Hematology & Medical Oncology, Weil Cornell Medical College, New York, NY

⁵Department of Pharmacology, Boston University School of Medicine, Boston, MA

⁶Department of Neurology, Children's Hospital Colorado

DOI: 10.1523/ENEURO.0020-15.2016

Received: 1 March 2015

Revised: 22 January 2016

Accepted: 28 January 2016

Published: 10 February 2016

Author Contributions: A.X.T., M.I.G., A.J.C., J.C., S.J.R., and A.B.-K. designed research; A.X.T., Y.C.D.A., A.J.C., J.C., and P.L. performed research; A.X.T., Y.C.D.A., and A.B.-K. analyzed data; A.X.T., M.I.G., B.L.H., and A.B.-K. wrote the paper; B.L.H. contributed unpublished reagents/analytic tools.

Funding: NINDS: 5R01NS051710. NINDS: 5R01NS030687. NINDS: F31NS078844. NINDS: P30NS048154. NIH/NCRR: UL1 RR025780. Epilepsy Foundation/ American Epilepsy Society;

Conflict of Interest: Authors report no conflict of interest.

NIH/NINDS, Epilepsy Foundation/American Epilepsy Society, NIH/NCRR

Correspondence should be addressed to Amy Brooks-Kayal, E-mail: Amy.Brooks-Kayal@childrenscolorado.org

Cite as: eNeuro 2016; 10.1523/ENEURO.0020-15.2016

Alerts: Sign up at eneuro.org/alerts to receive customized email alerts when the fully formatted version of this article is published.

Accepted manuscripts are peer-reviewed but have not been through the copyediting, formatting, or proofreading process.

This is an open-access article distributed under the terms of the Creative Commons Attribution 4.0 International (<http://creativecommons.org/licenses/by/4.0>), which permits unrestricted use, distribution and reproduction in any medium provided that the original work is properly attributed.

eNeuro

<http://eneuro.msubmit.net>

eN-NWR-0020-15R2

Rapid increases in ProBDNF after pilocarpine-induced status epilepticus in mice are associated with reduced proBDNF cleavage machinery

1. Manuscript Title

Rapid increases in proBDNF after pilocarpine-induced status epilepticus in mice are associated with reduced proBDNF cleavage machinery

2. Abbreviated Title

ProBDNF is acutely elevated post-status epilepticus

3. List all Author Names and Affiliations in order as they would appear in the published article

Ajay X. Thomas^{1,2,3}, Yasmin Cruz Del Angel¹, Marco I. Gonzalez^{1,2}, Andrew J. Carrel^{1,2}, Jessica Carlsen¹, Philip M. Lam¹, Barbara L. Hempstead⁴, Shelley J. Russek⁵, Amy R. Brooks-Kayal^{1,2,6}; ¹Department of Pediatrics, University of Colorado Anschutz Medical Campus, Aurora, CO; ²Neuroscience Program, University of Colorado Anschutz Medical Campus, Aurora, CO; ³Medical Scientist Training Program; University of Colorado Anschutz Medical Campus, Aurora, CO; ⁴Departments of Medicine, Hematology & Medical Oncology, Weil Cornell Medical College, New York, NY; ⁵Department of Pharmacology, Boston University School of Medicine, Boston, MA; ⁶Department of Neurology, Children's Hospital Colorado.

4. Author Contributions:

AXT Designed and Performed research, Analyzed data, and Wrote the paper; YC Designed and Performed research, Analyzed data and edited paper; AJC and JC Designed and Performed research, and edited paper; PL Performed research. MIG Designed research and edited the paper; BLH Contributed reagents, protocols, and discussion; SJR Designed research and edited paper; ABK Designed research, Analyzed data and Wrote the paper.

5. Correspondence should be addressed to (include email address)

Amy Brooks-Kayal <Amy.Brooks-Kayal@childrenscolorado.org>

6. Number of Figures

8

7. Number of Tables

1

8. Number of Multimedia

0

9. Number of words for Abstract 250**10. Number of words for Significance Statement** 104**11. Number of words for Introduction** 750**12. Number of words for Discussion**

1,388

13. Acknowledgements

We thank Dana Hund and Radu Moldovan for their assistance with completion of these studies. The studies were supported by NINDS funding: 5R01NS051710 to ABK and SJR, 5R01NS030687 to BLH, F31NS078844 to AXT, and by Epilepsy Foundation/American Epilepsy Society funding to AXT. Imaging experiments were performed in the University of Colorado Anschutz Medical Campus Advance Light Microscopy Core supported in part by Rocky Mountain Neurological Disorders Core Grant Number P30NS048154 and by NIH/NCRR Colorado CTSI Grant Number UL1 RR025780.

14. Conflict of Interest

Authors report no conflict of interest

15. Funding sources

NIH/NINDS, Epilepsy Foundation/American Epilepsy Society, NIH/NCRR

1 **Abstract**

2 Brain-derived neurotrophic factor (BDNF) levels are elevated after status epilepticus (SE),
3 leading to activation of multiple signaling pathways, including the janus kinase/signal transducer
4 and activator of transcription (JAK/STAT) pathway that mediates a decrease in GABA_A receptor
5 (GABA_AR) α 1- subunits in the hippocampus (Lund et al., 2008). While BDNF can signal via its
6 pro- or mature form, the relative contribution of these forms to signaling after SE is not fully
7 known. In the current study, we investigate changes in proBDNF levels acutely after SE in
8 C57BL/6J mice. In contrast to previous reports (Unsain et al., 2008; Volosin et al., 2008;
9 VonDran et al., 2014), our studies found that levels of proBDNF in the hippocampus are
10 markedly elevated as early as three hours after SE onset and remain elevated for seven days.
11 Immunohistochemistry studies indicate that seizure-induced BDNF localizes to all hippocampal
12 subfields, predominantly in principal neurons and also astrocytes. Analysis of the proteolytic
13 machinery that cleaves proBDNF to produce mature BDNF demonstrates that acutely after SE
14 there is a decrease in tissue plasminogen activator (tPA) and an increase in plasminogen
15 activator inhibitor-1 (PAI-1), an inhibitor of extracellular and intracellular cleavage, which
16 normalizes over the first week after SE. *In vitro* treatment of hippocampal slices from animals
17 24 hours after SE with a PAI-1 inhibitor reduces proBDNF levels. These findings suggest that
18 rapid proBDNF increases following SE are due in part to reduced cleavage, and that proBDNF
19 may be part of the initial neurotrophin response driving intracellular signaling during the acute
20 phase of epileptogenesis.

21

22 **Significance Statement**

23 The studies reported here are the first to demonstrate acute changes in the expression of
24 proBDNF within three hours of onset of status epilepticus (SE) onset that occur within principle
25 cells and glia in all hippocampal subfields. We further found evidence that reduced expression

26 of tPA, part of the extracellular proteolytic cascade, and increased expression of plasminogen
27 activator inhibitor-1 (PAI-1), an inhibitor of extracellular and intracellular cleavage, may
28 contribute to reduced proBDNF cleavage and elevations in proBDNF levels. These findings
29 suggest that proBDNF may be part of the initial neurotrophin response driving intracellular
30 signaling acutely after SE and during the earliest phase of epileptogenesis.

31

32 **Introduction**

33 Brain-derived neurotrophic factor (BDNF) promotes growth and differentiation of neurons during
34 development and plays an important role in many physiological processes, such as learning and
35 memory, as well as various pathological processes, such as epileptogenesis (Lu et al., 2014).

36 Synthesis and expression of BDNF are highly regulated throughout the nervous system

37 (Lessmann and Brigadski, 2009). BDNF is initially synthesized as a precursor protein

38 (preproBDNF) in the endoplasmic reticulum and is transported to the Golgi as proBDNF once

39 the signal peptide is cleaved. Mature BDNF can be produced intracellularly by furin-mediated

40 cleavage or by proprotein convertase in immature secretory granules (Mowla et al., 1999).

41 ProBDNF can also be cleaved extracellularly by matrix metalloproteinases (MMP -3, -7, or 9), or

42 by components of the tissue plasminogen activator/plasmin (tPA/plasmin) proteolytic cascade

43 (Lee et al., 2001; Pang et al., 2004). The activity of these proteases is tightly regulated.

44 Plasminogen activator inhibitor-1 (PAI-1) inhibits both tPA and furin, inhibiting both extracellular
45 and intracellular cleavage (Binder et al., 2002; Dupont et al., 2009; Bernot et al., 2011; figure 1).

46 In addition, tissue inhibitor of metalloproteinases (TIMPs) inhibit MMPs while neuroserpin and

47 α 2 antiplasmin (A2AP) inhibit the tPA/plasmin proteolytic cascade (Hastings et al., 1997;

48 Krueger et al., 1997; Brew et al., 2000; Yepes and Lawrence, 2004; Coughlin, 2005).

49

50 Several studies have demonstrated that a significant portion of BDNF protein is secreted as
51 proBDNF and cleaved extracellularly via the tPA/plasmin proteolytic cascade (Pang et al., 2004;
52 Nagappan et al., 2009). *In vitro*, high frequency neuronal activity triggers simultaneous release
53 of proBDNF and tPA to generate mBDNF extracellularly (Nagappan et al., 2009), suggesting
54 that this could occur *in vivo* after repeated neuronal firing that is observed during seizures.
55 However, the *in vivo* effects of acute seizures on proBDNF levels have not yet been fully
56 elucidated.

57

58 Numerous reports suggest that BDNF levels are increased in the hippocampus after seizures
59 induced by kindling (Ernfors et al., 1991), electroconvulsive shock (Altar et al., 2004), kainate
60 (Rudge et al., 1998), and pilocarpine (Roberts et al., 2006). In addition, several studies suggest
61 a pro-epileptogenic effect of BDNF that appears to be mediated at least in part by activation of
62 the tropomyosin-receptor kinase B (TrkB) receptors (McNamara et al., 2006). However, other
63 studies suggest that intrahippocampal infusion of BDNF results in enhanced resistance to
64 kindling and may protect against epileptogenesis (Larmet et al., 1995; Reibel et al., 2000).
65 These contrasting findings may be due, in part, to differential actions of proBDNF and mBDNF
66 during epileptogenesis.

67

68 A potential role for the proneurotrophins in epileptogenesis is starting to emerge. Enhancing
69 cleavage of pro-nerve growth factor (proNGF) to generate mature NGF provides
70 neuroprotection after administration of kainate to organotypic slice cultures (Le and Friedman,
71 2012). In rodents, increases in BDNF mRNA occur as early as three hours after pilocarpine-
72 induced status epilepticus (SE) (Mudò et al., 1996) and increased proBDNF has been detected
73 24 hours after SE induction (Volosin et al., 2008; VonDran et al., 2014). More recently, it has
74 been reported that high-dose proBDNF applied to cultured hippocampal neurons may cause
75 alterations in GABAergic neurotransmission by promoting GABA_AR endocytosis and

76 degradation through activation of the RhoA-Rock-PTEN pathway, and may contribute to
77 repression of GABA_AR synthesis through activation of the janus kinase/signal transducer and
78 activator of transcription (JAK/STAT) pathway (Riffault et al., 2014). Addition of exogenous
79 BDNF to neuronal cultures rapidly increases STAT3 phosphorylation (Ng et al., 2006; Lund et
80 al., 2008). BDNF-dependent activation of the JAK/STAT pathway in rat dentate gyrus occurs
81 within six hours of SE onset and drives a decrease in mRNA for the $\alpha 1$ subunit of GABA_AR
82 (Lund et al., 2008; Grabenstatter et al., 2014), suggesting that BDNF-induced activation of the
83 JAK/STAT pathway occurs rapidly after SE onset.

84

85 To better understand the potential contribution of proBDNF during the earliest phases of
86 epileptogenesis, we utilized proBDNF specific antibodies in wild-type C57BL/6J mice and
87 knock-in mice on a C57BL/6J background that express a hemagglutinin-tagged BDNF
88 transgene under the control of endogenous *bdnf* promoters (Yang et al., 2009) to assess the
89 levels and localization of BDNF acutely following the induction of pilocarpine-induced SE. The
90 study finds that within the first three hours after SE onset there is an acute increase in proBDNF
91 levels in principal neurons and glia in all hippocampal subfields, as well as altered expression of
92 both tPA and PAI-1 that would be predicted to reduce proBDNF cleavage. Taken together
93 these data suggest that reduced BDNF cleavage acutely after SE leads to proBDNF
94 accumulation, which may be the initial neurotrophin driving cell signaling during early
95 epileptogenesis.

96

97 **Materials & Methods**

98 **Induction of SE:**

99 All animal procedures were performed in accordance with the authors' institutional animal care
100 and use committee's regulations and NIH Guidelines, "Guide for the care and use of laboratory

101 animals". Adult male animals were utilized for all studies and were group housed with up to five
102 age-matched littermates in temperature and humidity controlled rooms with access to food and
103 water *ad libitum* on a 12 hour light/dark cycle.

104

105 Knock-in mice that express a *bdnf* allele with a hemagglutinin tag added to the C-terminus of the
106 murine coding exon of BDNF (BDNF-HA) were generously provided by the Hempstead group
107 (Weill Cornell Medical College) (Yang et al., 2009). BDNF-HA mice were backcrossed on a
108 C57BL/6J background for more than ten generations. Wild-type (WT) C57BL/6J mice (Jackson
109 Laboratory) were utilized for studies with proBDNF antibody detection and the protease
110 machinery studies. SE was induced using repetitive intraperitoneal (i.p.) injections of pilocarpine
111 as previously described (Müller et al., 2009). The mice acquired from Jackson Laboratory were
112 received at five weeks of age and allowed to rest for one week prior to handling in order to
113 acclimate to the environment and altitude. Six- to eight-week-old WT and BDNF-HA mice (18-
114 24g) were handled for at least one week to reduce the stress produced by handling required for
115 induction of SE. The induction protocol was initiated between 7:00-8:00AM to minimize diurnal
116 variation. The mice were transferred to the induction room, marked, weighed, and allowed to
117 rest undisturbed for at least one hour. To block the peripheral muscarinic effects of pilocarpine,
118 each mouse was given an i.p. injection of 1mg/kg scopolamine methyl bromide (Sigma) fifteen
119 minutes before the first pilocarpine injection on the day of seizure induction. An initial dose of
120 pilocarpine HCl (200mg/kg, Sigma) was given, then one hour after the first injection subsequent
121 doses (100mg/kg) were given at 30 min intervals. The animals were group housed with up to
122 five age-matched littermates and then separated into individual cages after the third injection for
123 individual monitoring of behavioral seizures. Injections were discontinued at the onset of SE,
124 which was defined by the appearance of repeated behavioral seizures (stage four or higher with
125 at least one seizure being five or higher) according to a modified Racine scale (Borges et al.,
126 2003).

127

128 SE typically initiated approximately three hours after the first injection, requiring at least three
129 injections (400mg/kg total dose) of pilocarpine with an average of five injections (600mg/kg total
130 dose) of pilocarpine. SE persisted for at least 90 minutes with approximately 30% of animals
131 successfully undergoing SE and surviving until their respective time points. The specific cause
132 of death cannot be definitively determined but post-convulsion respiratory failure appeared to be
133 a common cause of acute death after pilocarpine administration (as has been previously
134 described; Boyd and Fulford, 1961). Control mice were given injections of saline at identical
135 time intervals. Mice that were sacrificed more than three hours after SE induction were returned
136 to their housing room and given free access to water, Gatorade, and moistened chow with equal
137 parts sucrose. Mice were sacrificed with rapid isoflurane-induced anesthesia followed by
138 decapitation. Fresh tissue for western blot was collected via rapid hippocampal dissection in ice
139 cold PBS containing phosphatase inhibitors (phosphatase inhibitor cocktail 2, P5726, Sigma)
140 and frozen on dry ice. The two hippocampi from each animal were pooled into a single sample
141 for that animal, and samples were stored at -80°C until lysate preparation. For
142 immunohistochemistry, mice were sacrificed at three hours after SE onset by deep anesthesia
143 with ketamine/xylazine and inhaled isoflurane followed by rapid intracardiac perfusion with ice
144 cold PBS then 4% paraformaldehyde in phosphate buffer pH 7.4. The brains were dissected
145 out, postfixed overnight in 4% paraformaldehyde and underwent cryoprotection in 30% sucrose
146 in PBS, and were then stored at -80°C in Tissue-Tek® O.C.T. Compound (Sakura Finetek,
147 Torrance, CA) until sectioning.

148

149 **Western blotting:** The frozen hippocampi were lysed in RIPA buffer (50mM Tris-HCl, pH 7.4,
150 150mM NaCl, 0.25% deoxycholic acid, 1% NP-40, 1mM EDTA) with 10mM
151 phenylmethylsulfonyl fluoride, 10mM sodium orthovanadate, 10mM sodium fluoride,
152 phosphatase inhibitor cocktail 2 (1:250) and protease inhibitor cocktail (1:250, P8340, Sigma)

153 using an ultrasonic sonifier. Samples were then gently shaken at 4°C for 30 minutes and
154 centrifuged at 14,000 x g for 30 minutes at 4°C. The supernatants were reserved, aliquoted, and
155 stored at -80°C until sodium dodecyl sulfate polyacrylamide gel electrophoresis (SDS-PAGE).
156 Identical amounts of protein were loaded per lane for each sample on all blots probed with a
157 given antibody, with 20-60ug of protein utilized depending on the specific antibody used. After
158 gel transfer, the nitrocellulose membranes were blocked with 5% milk (furin and MMP-9 were
159 blocked with 5% non-fat dry milk, 2% BSA, 4% FBS, 4% normal horse serum, and 4% normal
160 goat serum). The blots probed with the anti-HA and BDNF antibody were first washed with Tris-
161 buffered saline with Tween-20 (TBST, 50mM Tris-Base, 150mM NaCl, 0.05% Tween-20, pH
162 7.6) and then fixed with 2.5% glutaraldehyde in PBS, washed twice with PBS, washed twice
163 with TBST, and then blocked with 5% milk in TBST. All membranes were incubated overnight at
164 4°C with their respective primary antibody in diluted blocking buffer. The following antibodies
165 and concentrations were used: mouse monoclonal HA.11 clone 16B12 antibody (1:3,000, MMS-
166 101P, Covance), mouse monoclonal proBDNF antibody (1:1000, H10001G-MA, GeneCopeia),
167 rabbit polyclonal to alpha-2 antiplasmin (1:2,000, ab62771, Abcam), rabbit polyclonal furin
168 antibody (1:1,000, sc-20801, Santa Cruz), rabbit polyclonal MMP-9 antibody (1:2,000, AB13458,
169 Millipore), sheep polyclonal neuroserpin antibody (1:2,000, SASMNSP-GF-HT, Molecular
170 Innovations), rabbit polyclonal PAI-1 antibody (1:1,000, ASMPAI-GF-HT, Molecular
171 Innovations), rabbit polyclonal plasminogen antibody (1:3,000, ASMPLG-GF-HT, Molecular
172 Innovations), sheep polyclonal tPA antibody (1:500, SASTPA-GF-HT, Molecular Innovations),
173 and rabbit polyclonal TIMP-1 antibody (1:1,000, AB770, Millipore). Following incubation with the
174 appropriate secondary antibody, membranes were incubated with SuperSignal West Dura
175 Chemiluminescent Substrate (Pierce) with the anti-HA blots being enhanced with Lumigen
176 TMA-6 (Lumigen). Blots were stripped with 50mM glycine (pH 2.3) and reprobbed with other
177 primary antibodies or Actin (1:20,000-80,000, A2066, Sigma). Western blotting results
178 presented include representative images of the blots run in duplicate and adjusted for contrast

179 and the densitometry quantitation of each band normalized to actin that was used as a loading
180 control to ensure consistent protein amounts were loaded across samples using FIJI (Schindelin
181 et al., 2012). The average of the normalized densitometry measurements for the control group
182 was considered 100% with error bars reported as S.E.M and N referring to the number of
183 samples consisting of lysates from both hippocampi from individual animals in each group.

184

185 **Immunohistochemistry:** Brains were sectioned at 30 μm into cryoprotectant (30% sucrose,
186 30% ethylene glycol, and 0.1M phosphate buffer) and stored at -20°C for floating section
187 staining. Sections were washed in PBS several times and then blocked with 3% BSA, 3%
188 normal goat serum, and 3% normal donkey serum with 0.1% Triton X-100 in PBS for one hour
189 at room temperature and then incubated overnight at 4°C with rabbit polyclonal HA antibody
190 (1:500, A6908, Sigma) in combination with chicken polyclonal MAP2 antibody (1:1000, ab5392,
191 Abcam) and guinea pig polyclonal GFAP antibody (1:500, 174004, Synaptic Systems). After
192 primary antibody washing, sections were incubated for one hour with a biotinylated goat anti-
193 rabbit IgG secondary antibody (1:400, 111-065-144, Jackson Immunoresearch), a goat anti-
194 chicken IgY Alexa Fluor 568, and donkey anti-guinea pig IgG Alexa Fluor 647 to detect MAP2
195 and GFAP, respectively. Sections were subsequently incubated for one hour with Alexa Fluor
196 488-Streptavidin (1:800, 016-580-084, Jackson Immunoresearch) to visualize the HA tag. The
197 sections were mounted on glass slides with VECTASHIELD mounting medium with DAPI
198 (Vector Labs), coverslipped, and sealed.

199

200 **Confocal microscopy:** Slide-mounted sections of immunolabeled hippocampi were viewed on
201 an inverted microscope (Axio Examiner Z1, Carl Zeiss) equipped with Plan-Apochromat 20x
202 (0.8 NA) or 63x (oil differential interference contrast; 1.4 NA) objectives and attached to a
203 spectral confocal laser system (LSM 780, Carl Zeiss) powered by ZEN 2012 software (Carl
204 Zeiss). The tissue was scanned at room temperature with a tunable infrared Coherent

205 Chameleon Ultra II laser tuned to 800nm to detect DAPI staining and 488-, 561-, and 633-nm
206 laser lines to detect the Alexa fluorophores 488, 568, and 647, respectively. Images were
207 acquired as z-stacks using sequential line (mean of four) scanning. Colocalization of two
208 fluorophores with DAPI was simultaneously qualitatively assessed in the x, y, and z planes of
209 each optical section. Average projection images of 5 optical slices spaced 2um in the z-axis
210 were produced and minimal adjustments to image contrast and intensity were made in FIJI
211 (Schindelin et al., 2012) using the levels or contrast/brightness functions. All brains and sections
212 were processed in parallel with images acquired, adjusted and analyzed in an identical manner
213 between SE and control animals. Images were arranged and annotated using Adobe Illustrator
214 (Adobe Corporation).

215

216 **Acute Hippocampal Section Studies.** Animals were anesthetized with isoflurane, sacrificed,
217 the brain swiftly removed, and placed in cold (4°C) oxygenated (95% O₂, 5% CO₂) sucrose-
218 modified aCSF containing (in mM): Sucrose (45), NaCl (87), glucose (25), NaHCO₃ (25), KCl
219 (2.5), NaH₂PO₄ (1.25), MgCl₂ (7), and CaCl₂ (0.5), pH 7.4 and 300–310 mOsm. Transverse
220 hippocampal slices (300 μm) were obtained using a slicing vibratome (Leica VT1200s).
221 Hippocampi were dissected out from slices in the cold sucrose-modified aCSF solution and
222 rinsed briefly in oxygenated aCSF containing (in mM): NaCl (130), Glucose (10), NaHCO₃ (25),
223 KCl (3.5), NaH₂PO₄ (1.25), MgCl₂ (2), CaCl₂ (2), pH 7.4 and 300–305 mOsm. Rinsed slices
224 were then placed on ice in a 6-well plate with 5 mL of aCSF in individual wells modified to allow
225 delivery of oxygen. Alternating slices from the two hippocampi from a single animal were placed
226 in wells for the vehicle or PAI-1 inhibitor group and care was taken to assure that a similar
227 number of sections from each hippocampus was placed in each well. Once sectioning was
228 completed, 25 μL of vehicle (DMSO, Sigma Aldrich) was added to one of the wells (vehicle
229 group) and 25 μL of the PAI-1 inhibitor Tiplaxtinin (Axon 1383) (74 mM stock in DMSO) was
230 added to the other well (final concentration 370 μM; Axon Medchem). Both the vehicle and

231 inhibitor wells were carefully mixed with repeated aspiration to obtain equal distribution in the
 232 aCSF. Once the vehicle and inhibitor were added, the 6-well plate was placed into a water bath
 233 and incubated at 36°C for 4 hours with constant, low pressure oxygenation. After incubation,
 234 slices were collected, flash frozen using dry ice, and stored at -80°C until lysate preparation.

235

236 **Statistical Table**

	Data Structure	Type of Test	Power
Figure 2a. Increased proBDNF 3h post-SE (HA- immunoreactivity)	Normal distribution	Student T-test	0.9775
Figure 2b. Increased proBDNF 24h post-SE (HA- immunoreactivity)	Normal distribution	Student T-test	0.9917
Figure 3a. Increased proBDNF 3h post-SE (Commercial BDNF antibodies)	Normal distribution	Student T-test	1.0000
Figure 3b. Increased proBDNF 24h post-SE (Commercial BDNF antibodies)	Normal distribution	Student T-test	0.9104
Figure 5a. No change in furin 3h post-SE	Normal distribution	Student T-test	0.0511
Figure 5b. Significant increase in furin 24h post-SE	Normal distribution	Student T-test	0.9198
Figure 5c. No change in plasminogen 3h post-SE	Normal distribution	Student T-test	0.5067
Figure 5d. No change in plasminogen 24h post-SE	Normal distribution	Student T-test	0.6526
Figure 5e. No change in MMP-9 3h post-SE	Normal distribution	Student T-test	0.1905
Figure 5f. No	Normal distribution	Student T-test	0.2765

change in MMP-9 24h post-SE			
Figure 5g. Significant reduction in tPA 3h post-SE	Normal distribution	Student T-test	0.9394
Figure 5h. Significant reduction in tPA 24h post-SE	Normal distribution	Student T-test	1.0000
Figure 6a. No change in A2AP 3h post-SE	Normal distribution	Student T-test	0.5646
Figure 6b. No change in A2AP 24h post-SE	Normal distribution	Student T-test	0.1068
Figure 6c. Reduction in neuroserpin at 3h post-SE.	Normal distribution	Student T-test	0.9961
Figure 6d. No change in neuroserpin at 24h post-SE	Normal distribution	Student T-test	0.0744
Figure 6e. No change in 23kDa non-glycosylated TIMP-1 at 3h post- SE	Normal distribution	Student T-test	0.1867
Figure 6e. No change in 28kDa glycosylated TIMP- 1 at 3h post-SE	Normal distribution	Student T-test	0.5007
Figure 6f. No change in 23kDa non-glycosylated TIMP-1 at 24h post- SE	Normal distribution	Student T-test	0.6078
Figure 6f. Significant reduction in 28kDa glycosylated TIMP-1 at 24h post-SE	Normal distribution	Student T-test	0.9987
Figure 6g. Significant increase in PAI-1 at 3h post- SE	Normal distribution	Student T-test	0.9601
Figure 6h. Significant increase in PAI-1 at 24h post-SE	Normal distribution	Student T-test	1.0000
Figure 7a.	Normal distribution	Student T-test	0.971

Increased proBDNF 3d post-SE (Commercial BDNF antibodies)				237
				238
Figure 7a. Increased proBDNF 7d post-SE (Commercial BDNF antibodies)	Normal distribution	Student T-test	1.000	239
				240
				241
Figure 7b. Increased PAI-1 3d post-SE (Commercial BDNF antibodies)	Non-normal distribution	Mann Whitney test	N/A	242
				243
Figure 7b. No change in PAI-1 7d post-SE (Commercial BDNF antibodies)	Normal distribution	Student T-test	0.985	244
				245
				246
Figure 7c. No change in tPA 3d post-SE (Commercial BDNF antibodies)	Normal distribution	Student T-test	0.981	247
				248
Figure 7c. Increased tPA 7d post-SE (Commercial BDNF antibodies)	Normal distribution	Student T-test	1.000	249
				250
				251
Figure 8. PAI-1 Inhibition reduces proBDNF levels after pilocarpine SE	N/A	Paired T-test	0.995	252
				253

254 **Res**255 **ults**

256 Levels of proBDNF protein expression were initially assessed in whole hippocampal lysates
 257 from age-matched pilocarpine- and saline-treated WT C57BL/6J mice using a mouse
 258 monoclonal antibody specific for proBDNF (GeneCopoeia). A significant increase in the
 259 immunoreactivity of proBDNF was observed at three (figure 2a; control- 100.0 ± 10.6 N=5 vs SE-
 260 326.4 ± 12.2 N=5, t-test $p < 0.001$) and 24 hours (figure 2b; 100.0 ± 16.6 N=4 vs 180.4 ± 18.0
 261 N=4, t-test $p < 0.05$) after SE onset. These data suggest that a significant increase in proBDNF
 262 protein levels occurs as soon as three hours after pilocarpine-induced SE.

263

264 To further assess proBDNF levels and cellular localization, we used knock-in mice that express
265 a *bdnf* allele with a hemagglutinin tag added to the C-terminus of the murine coding exon of
266 BDNF (BDNF-HA). Tissue from control BDNF-HA mice (controls) or BDNF-HA mice subjected
267 to pilocarpine induced SE was collected at three and 24 hours after SE onset. Western blot
268 analysis showed a significant increase in proBDNF corresponding to a 34kD HA-
269 immunoreactive band as early as three hours after SE induction (figure 3a; control- $100.0 \pm$
270 20.5 , N=3 vs SE- 300.4 ± 37.4 N=6; t-test $p < 0.01$). In addition, a significant increase in
271 proBDNF immunoreactivity was also observed 24 hours after SE (figure 3b; control- $100.0 \pm$
272 29.3 N=3 vs SE- 610.1 ± 89.7 N=6; t-test $p < 0.01$). In contrast, no difference in HA-
273 immunoreactivity was observed for the 14 kD band corresponding to mBDNF between SE and
274 control animals at either time point (figure 3a&b; three hours: control- 100.0 ± 12.2 (N=3) vs SE-
275 96.4 ± 5.8 (N=6); 24 hours: control- 100.0 ± 4.9 (N=3) vs SE- 98.5 ± 5.0 (N=6); t-test $p > 0.05$ at
276 both time points). Together, these data provide further evidence that a significant increase in
277 the levels of proBDNF are triggered acutely after SE onset.

278

279 To determine the cellular distribution of BDNF protein after SE, HA immunoreactivity was
280 analyzed in coronal sections co-labeled with a neuronal (MAP2) and an astrocytic (GFAP)
281 marker (figure 4). It is important to note that the HA immunostaining is unable to distinguish
282 between proBDNF and mBDNF, therefore in these experiments the signal detected was
283 considered as total BDNF expression. Another important limitation of these findings is that one
284 cannot distinguish between HA immunoreactivity indicating the site of BDNF pre-release or
285 internalization. Co-localization of HA and MAP2 immunoreactivity was assessed to identify
286 BDNF expression in neurons and co-localization of HA and GFAP immunoreactivity was
287 assessed to identify BDNF expression in astrocytes. The observed pattern of protein expression
288 detected in control animals is consistent with the pattern of expression previously reported by

289 others using the same HA-tagged BDNF knock-in mice (Yang et al., 2009; Dieni et al., 2012).
290 The most prominent HA immunoreactivity signal is detected in the mossy fiber pathway, CA3
291 pyramidal neurons and CA1 pyramidal neurons (figure 4). When compared to controls, mice at
292 three hours post-SE showed an increase in HA immunoreactivity as well as MAP2
293 immunoreactivity that can be detected in all hippocampal regions analyzed. In SE animals, the
294 pattern of HA immunoreactivity is well co-localized with both MAP2 (figure 4a&b) and GFAP
295 immunostaining (figure 4a&c), suggesting that within the hippocampus of animals acutely
296 following SE, BDNF is localized in principal neurons and astrocytes.

297

298 The very rapid elevation of proBDNF levels detected by western blot suggests that in addition to
299 the previously documented increase in BDNF expression, the typically rapid cleavage of
300 proBDNF might also be impaired after SE. Therefore, expression of enzymes involved in
301 proBDNF cleavage were analyzed via western blot (n=5 for each group at three hours and n=4
302 for each group at 24 hours for all assays). Our analyses showed that there is no statistical
303 difference in furin immunoreactivity three hours after SE (figure 5a; control- 100.0 ± 6.5 vs SE-
304 99.9 ± 5.7 ; t-test $p>0.05$) while there is a modest but significant increase in furin expression at
305 24 hours after SE (figure 5b; control- 100.0 ± 2.202 vs SE- 115.1 ± 3.970 ; t-test $p<0.05$). In
306 contrast, there is no statistical difference in the immunoreactivity of plasminogen observed at
307 three (figure 5c; control- 100.0 ± 5.4 vs SE- 113.4 ± 5.0 ; t-test $p>0.05$) or 24 hours after SE
308 (figure 5d; control- 100.0 ± 11.76 vs SE- 136.8 ± 10.8 ; t-test $p>0.05$). In addition, there is no
309 statistical difference in the immunoreactivity of MMP-9 observed at three (figure 5e; control-
310 100.0 ± 3.7 vs SE- 104.4 ± 3.7 ; t-test $p>0.05$) or 24 hours after SE (figure 5f; control- $100.0 \pm$
311 6.9 vs SE- 112.5 ± 8.0 ; t-test $p>0.05$). Interestingly, a significant decrease in tPA expression
312 was observed at both three (figure 5g; control- 100.0 ± 9.3 vs SE- 66.3 ± 2.4 ; t-test $p<0.01$) and
313 24 hours (figure 5h; control- 100.0 ± 5.9 vs SE- 47.9 ± 2.7 ; t-test $p<0.001$) after SE.

314

315 In order to further investigate the mechanism of proBDNF cleavage after SE, the levels of
316 protease inhibitors known to inhibit activity of proBDNF cleavage enzymes were analyzed. We
317 observed no change in the immunoreactivity of A2AP, an inhibitor of plasmin activity, at three
318 (figure 6a; control- 100.0 ± 4.8 vs SE- 110.2 ± 1.9 ; t-test $p > 0.05$) or 24 hours after SE (figure 6b;
319 control- 100.0 ± 6.0 vs SE- 96.4 ± 5.3 ; t-test $p > 0.05$). A slight reduction in the immunoreactivity
320 of neuroserpin, a known inhibitor of tPA activity, was observed at three hours after SE (figure
321 6c; control- 100.0 ± 2.2 vs SE- 72.3 ± 5.4 ; t-test $p < 0.01$) but not at 24 hours after SE (figure 6d;
322 control- 100.0 ± 2.7 vs SE- 101.0 ± 3.6 ; t-test $p > 0.05$). As seen in figure 6e&f, two forms of
323 TIMP-1, an inhibitor of MMP activity, can be detected via western blot, a 23kDa non-
324 glycosylated and a 28kDa glycosylated form. There is no statistical difference in the
325 immunoreactivity of the non-glycosylated form at three (figure 6e; control- 100.0 ± 6.1 vs SE-
326 93.3 ± 5.4 ; t-test $p > 0.05$) or 24 hours after SE (figure 6f; control- 100.0 ± 4.9 vs SE- 86.41 ± 3.9 ;
327 t-test $p > 0.05$). In addition, there is no statistical difference in the immunoreactivity of the
328 glycosylated form at three hours after SE (figure 6e; control- 100.0 ± 7.9 vs SE- 85.0 ± 2.6 ; t-test
329 $p > 0.05$); however, there is a significant reduction at 24 hours after SE (figure 6f; control- $100.0 \pm$
330 5.0 vs SE- 65.4 ± 4.1 ; t-test $p < 0.01$). Most notably, there is a robust increase in the
331 immunoreactivity of PAI-1, an inhibitor of both furin and tPA, at three (figure 6g; control- $100.0 \pm$
332 13.1 vs SE- 183.8 ± 18.2 ; t-test $p < 0.01$) and 24 hours after SE (figure 6h; control- 100.0 ± 12.3
333 vs SE- 590.8 ± 63.3 ; t-test $p < 0.001$).

334

335 To determine if changes in the levels of proBDNF, PAI-1 and tPA persisted beyond 24 hours
336 after SE, levels of these proteins were examined at three and seven days following SE in wild-
337 type C57BL/6J mice. As can be seen in figure 7a, mean proBDNF level appears to peak at
338 three days following SE, although there is more variability at this time point than at earlier time
339 points (figure 7a: control- 100.0 ± 31.8 vs SE- 437.0 ± 122.0 ; t-test $p < 0.05$). At seven days
340 post-SE, proBDNF levels remain elevated, but the relative increase versus control is less than

341 at three days and variability is lower (figure 7a: control- 100.0 ± 18.8 vs SE- 222.0 ± 28.5 ; t-test
342 $p < 0.05$). PAI-1 levels are variable but overall remain elevated at three days (figure 7b: control-
343 100.0 ± 9.4 vs SE- 345.0 ± 117.8 ; Mann-Whitney test, $p < 0.05$), and have returned to control
344 levels at seven days (figure 7b: control- 100.0 ± 5.8 vs SE- 94.0 ± 4.0 ; t-test $p > 0.05$). Of note,
345 the same two samples showed very high levels of proBDNF and PAI-1, and interestingly these
346 two samples both came from animals that had extremely severe SE (multiple stage six
347 seizures). Levels of tPA were not different from controls at three days after SE (figure 7c;
348 control- 100.0 ± 9.2 vs SE- 116.0 ± 8.6 ; t-test $p > 0.05$), and were elevated compared to controls
349 at seven days after SE (figure 7c: control- 100.0 ± 5.0 vs SE- 149.0 ± 6.0 ; t-test $p < 0.001$).

350

351 To better assess if there was a causal relationship between elevated PAI-1 levels and increased
352 proBDNF after SE, we examined the effect of PAI-1 inhibition on proBDNF levels in
353 hippocampal slices from wild-type C57BL/6J mice 24 hours after SE. Hippocampal slices were
354 rapidly removed and incubated for 4 hours in aCSF containing the PAI-1 inhibitor tiplaxtinin (370
355 μM) or vehicle (DMSO). Tiplaxtinin treatment resulted in a significant reduction in proBDNF
356 levels compared to vehicle treatment in slices from 4 out of the 5 animals (figure 8; $p < 0.05$,
357 paired two-tailed t-test), suggesting that a reduction in proBDNF cleavage due to increased PAI-
358 1 may be contributing to elevation of proBDNF levels acutely after SE.

359

360 Discussion

361 These studies provide evidence for an increase in the levels of proBDNF acutely following the
362 induction of SE. In WT C57BL/6J mice as well as in HA-epitope tagged BDNF knock-in
363 C57BL/6J mice there is an increase in proBDNF as early as three hours after SE onset, with
364 levels remaining elevated at 24 hours and peaking at three days post-SE. The epitope tagged
365 knock-in C57BL/6J mice were further utilized to localize early increases in BDNF after SE and
366 HA-immunoreactivity was detected primarily in principal cells but also some astrocytes

367 throughout all hippocampal subfields. Finally, we demonstrated that acute increases in
368 proBDNF after SE are associated with changes in the enzymes involved in the proteolytic
369 processing of proBDNF (reduced tPA and increased PAI-1), and that enhancing proBDNF
370 cleavage by inhibiting PAI-1 reduces proBDNF levels in hippocampal slices from animals 24
371 hours post SE. Taken together these results suggest that inhibition of proBDNF cleavage
372 contributes to acute elevations of proBDNF within hours of SE onset, positioning proBDNF to
373 participate in early cell signaling events after SE such as activation of the JAK/STAT pathway.
374

375 Several groups have previously evaluated the levels of BDNF in epilepsy models (Ernfors et al.,
376 1991; Rudge et al., 1998; Altar et al., 2004; Roberts et al., 2006). The majority of these studies
377 quantitatively evaluated levels of mRNA but did not determine the levels of proBDNF and
378 mBDNF protein. A few studies have evaluated the levels of proBDNF and mBDNF after
379 seizures but none have reported an increase in proBDNF less than 24 hours after SE onset.
380 Unsain et. al analyzed the levels of BDNF following pilocarpine-induced SE in adult rats and
381 demonstrated an increase in proBDNF immunoreactivity three days after SE (Unsain et al.,
382 2008). Using immunohistochemistry, Volosin et. al reported an increase in proBDNF
383 immunoreactivity one day after pilocarpine-induced SE in rats (Volosin et al., 2008). Elevated
384 levels of proNGF protein have also been observed 24 hours after kainate-induced seizures *in*
385 *vivo* (Volosin et al., 2008; Le and Friedman, 2012). This increase in proNGF was not
386 accompanied by increases in mature NGF and resulted from inhibition of MMP-7 by TIMP-1 (Le
387 and Friedman, 2012). Most recently, it was reported that both proBDNF and mBDNF levels
388 were elevated 24 hours after single dose pilocarpine SE in 129SvJ mice (VonDran et al., 2014).
389

390 There may be a number of potential reasons why we were able to identify increases in proBDNF
391 earlier after SE than had been previously reported, including differences in the species (rats vs
392 mice), background strain (129SvJ vs. C57BL/6J), and model of SE (kainate or single high-dose

393 pilocarpine vs repeated low-dose pilocarpine). Repeating the studies utilizing the same
394 techniques on different models would help determine the effect of model selection on the
395 findings. Another distinction between the previous studies and the one presented here is the
396 use of BDNF-epitope tagged knock-in mice that allowed levels of BDNF protein to be probed
397 with high sensitivity and specificity.

398

399 To delineate the spatial expression of BDNF in response to SE, immunohistochemistry for HA
400 was combined with MAP2 and GFAP staining in BDNF-HA tagged mice to evaluate expression
401 in neurons and astrocytes, respectively. The pattern of immunoreactivity for total BDNF in
402 controls is similar to what has been previously reported by others (Dieni et al., 2012; VonDran et
403 al., 2014). BDNF immunoreactivity is increased three hours after SE and colocalizes with MAP2
404 and GFAP, demonstrating that acutely following SE proBDNF is expressed in principal neurons
405 and astrocytes in all hippocampal subfields. BDNF immunoreactivity is most strikingly elevated
406 in the cell bodies of principal neurons of CA3 and CA1 and the mossy fiber pathway.

407 Unfortunately, one is unable to determine if the BDNF localization corresponds with a site of
408 pre-release or internalization. One possibility to explain the presence of BDNF immunoreactivity
409 in non-neuronal cells is that the BDNF localized in the astrocytes may be due to internalization
410 since TrkB.T1 is located primarily in hippocampal astrocytes. The truncated Trk receptors can
411 function as a dominant-negative inhibitor by forming heterodimers with full-length TrkB leading
412 to internalization of BDNF and triggering clearance of BDNF and TrkB (Haapasalo et al., 2002).

413

414 To identify potential mechanisms leading to rapid elevations in proBDNF after SE, we examined
415 the expression of cleavage machinery known to process proBDNF into mBDNF. These studies
416 were based on the hypothesis that the observed rapid elevation in proBDNF levels may be due,
417 at least in part, to a reduction in proneurotrophin cleavage, akin to the inhibition of MMP-7
418 cleavage of proNGF reported to occur after kainate-induced SE in rats (Le and Friedman,

419 2012). Two potential mechanisms that could contribute to reduced proBDNF cleavage were
420 identified, a significant decrease in tPA levels and a robust increase in PAI-1 levels. The
421 tPA/plasmin proteolytic machinery is a major contributor to extracellular proBDNF cleavage, and
422 PAI-1 inhibits both furin and tPA, thereby inhibiting both intracellular and extracellular cleavage
423 of proBDNF. Elevation in levels of PAI-1 normally corresponds to depression in tPA activity. It is
424 thought that elevation of PAI-1 is an adaptive mechanism to attenuate excessive tPA activity
425 which can contribute to CNS pathology (Melchor and Strickland, 2005). In addition, theta burst
426 stimulation (14,400 pulses, 60 min) triggers simultaneous release of proBDNF and tPA to
427 generate mBDNF extracellularly *in vitro*, and exogenous administration of PAI-1 inhibited tPA
428 activity and attenuated conversion of proBDNF to mBDNF (Nagappan et al., 2009). Taken
429 together with our data demonstrating that PAI-1 inhibition with tiplaxtinin reduces proBDNF
430 levels in hippocampal slices from mice 24 hours after SE, these findings suggest that PAI-1 is a
431 major regulator of proBDNF conversion to mBDNF under both normal physiological conditions
432 and following seizures.

433

434 A limitation of the current study is that we were unable to fully evaluate mBDNF levels in parallel
435 with the changes in proBDNF. Unfortunately, in our hands significant intra-lot variability and
436 poor specificity were observed with commercial antibodies that reportedly identify mBDNF,
437 including the antibody used in the recent report by VonDran et al., and therefore studies using
438 mBDNF antibodies were not included in this report. Although we were able to identify clear and
439 specific bands at the reported sizes of both proBDNF and mBDNF on western blots of protein
440 lysates from BDNF-HA tagged mice reacted with an anti-HA antibody, due to difficulty breeding
441 we only had sufficient numbers of these mice to examine the earliest time points (three and 24
442 hours). Therefore, although we did not find evidence of an increase in mBDNF at these early
443 time points after SE, we were unable to confirm this with a secondary method (using mBDNF
444 antibody detection) and could not evaluate if mBDNF elevations occurred at later time points

445 after SE. An additional potential concern in using BDNF-HA tagged mice to follow endogenous
446 presence of BDNF is the possibility that the HA-tag may alter BDNF expression and/or
447 processing. This seems unlikely, however, as it has been previously reported that the HA-
448 tagged BDNF is expressed, processed and trafficked in the same manner as WT BDNF (Yang
449 et al., 2009, 2014).

450

451 The current study also does not investigate the downstream consequences of elevated
452 proBDNF levels following SE. The rapid increase in proBDNF after onset of SE is temporally
453 positioned to mediate BDNF-induced JAK/STAT activation that begins within an hour of SE
454 onset (Lund et al., 2008). Interestingly, high dose proBDNF has recently been reported to lead
455 to repression of GABA_AR synthesis in cultured hippocampal neurons *in vitro* through activation
456 of the JAK-STAT-ICER pathway (Riffault et al., 2014), suggesting that it might also mediate
457 JAK/STAT activation and subsequent GABA_AR α 1 subunit repression *in vivo* after SE. Thus,
458 further studies are required to fully understand the downstream molecular effects of the acute
459 elevation in proBDNF levels demonstrated in these studies and the role of proBDNF signaling in
460 epileptogenesis.

461

462 In summary, we demonstrate an increase in proBDNF levels that occur as early as three hours
463 after SE in principal neurons and their processes, as well as in astrocytes, throughout all
464 hippocampal subfields. We further present evidence that the elevation in proBDNF is due, at
465 least in part, to reductions in proBDNF cleavage that result from acute decreases in tPA
466 expression and increases in PAI-1, an inhibitor of both intracellular and extracellular proBDNF
467 cleavage. These findings suggest that proBDNF is highly abundant immediately following SE
468 onset and may be a key component of neurotrophin signaling during the earliest phases of
469 epileptogenesis.

470 **References**

- 471 Altar CA, Laeng P, Jurata LW, Brockman JA, Lemire A, Bullard J, Bukhman Y V, Young TA,
472 Charles V, Palfreyman MG (2004) Electroconvulsive seizures regulate gene expression of
473 distinct neurotrophic signaling pathways. *J Neurosci* 24:2667–2677.
- 474 Bernot D, Stalin J, Stocker P, Bonardo B, Scroyen I, Alessi M-C, Peiretti F (2011) Plasminogen
475 activator inhibitor 1 is an intracellular inhibitor of furin proprotein convertase. *J Cell Sci*
476 124:1224–1230.
- 477 Binder BR, Christ G, Gruber F, Grubic N, Hufnagl P, Krebs M, Mihaly J, Prager GW (2002)
478 Plasminogen activator inhibitor 1: physiological and pathophysiological roles. *News Physiol*
479 *Sci* 17:56–61.
- 480 Borges K, Gearing M, McDermott DL, Smith AB, Almonte AG, Wainer BH, Dingledine R (2003)
481 Neuronal and glial pathological changes during epileptogenesis in the mouse pilocarpine
482 model. *Exp Neurol* 182:21–34.
- 483 Boyd EM, Fulford RA (1961) Pilocarpine-Induced Convulsions And Delayed Psychotic-Like
484 Reaction. *Can J Biochem Physiol* 39:1287–1294.
- 485 Brew K, Dinakarandian D, Nagase H (2000) Tissue inhibitors of metalloproteinases: evolution,
486 structure and function. *Biochim Biophys Acta* 1477:267–283.
- 487 Coughlin PB (2005) Antiplasmin: the forgotten serpin? *FEBS J* 272:4852–4857.
- 488 Dieni S, Matsumoto T, Dekkers M, Rauskolb S, Lonescu MS, Deogracias R, Gundelfinger ED,
489 Kojima M, Nestel S, Frotscher M, Barde Y-A (2012) BDNF and its pro-peptide are stored in
490 presynaptic dense core vesicles in brain neurons. *J Cell Biol* 196:775–788.
- 491 Dupont DM, Madsen JB, Kristensen T, Bodker JS, Blouse GE, Wind T, Andreasen PA (2009)
492 Biochemical properties of plasminogen activator inhibitor-1. *Front Biosci (Landmark Ed*
493 *14:1337–1361.*
- 494 Ernfors P, Bengzon J, Kokaia Z, Persson H, Lindvall O (1991) Increased levels of messenger
495 RNAs for neurotrophic factors in the brain during kindling epileptogenesis. *Neuron* 7:165–
496 176.
- 497 Grabenstatter HL, Cruz Del Angel Y, Carlsen J, Wempe MF, White AM, Cogswell M, Russek
498 SJ, Brooks-Kayal AR (2014) The effect of STAT3 inhibition on status epilepticus and
499 subsequent spontaneous seizures in the pilocarpine model of acquired epilepsy. *Neurobiol*
500 *Dis* 62:73–85.
- 501 Haapasalo A, Sipola I, Larsson K, Åkerman KEO, Stoilov P, Stamm S, Wong G, Castrén E
502 (2002) Regulation of TRKB surface expression by brain-derived neurotrophic factor and
503 truncated TRKB isoforms. *J Biol Chem* 277:43160–43167.
- 504 Hastings GA, Coleman TA, Haudenschild CC, Stefansson S, Smith EP, Barthlow R, Cherry S,
505 Sandkvist M, Lawrence DA (1997) Neuroserpin, a brain-associated inhibitor of tissue
506 plasminogen activator is localized primarily in neurons. Implications for the regulation of
507 motor learning and neuronal survival. *J Biol Chem* 272:33062–33067.
- 508 Krueger SR, Ghisu GP, Cinelli P, Gschwend TP, Osterwalder T, Wolfer DP, Sonderegger P
509 (1997) Expression of neuroserpin, an inhibitor of tissue plasminogen activator, in the
510 developing and adult nervous system of the mouse. *J Neurosci* 17:8984–8996.
- 511 Larmet Y, Reibel S, Carnahan J, Nawa H, Marescaux C, Depaulis A (1995) Protective effects of
512 brain-derived neurotrophic factor on the development of hippocampal kindling in the rat.

- 513 Neuroreport 6:1937–1941.
- 514 Le AP, Friedman WJ (2012) Matrix metalloproteinase-7 regulates cleavage of pro-nerve growth
515 factor and is neuroprotective following kainic acid-induced seizures. *J Neurosci* 32:703–
516 712.
- 517 Lee R, Kermani P, Teng KK, Hempstead BL (2001) Regulation of cell survival by secreted
518 proneurotrophins. *Science* 294:1945–1948.
- 519 Lessmann V, Brigadski T (2009) Mechanisms, locations, and kinetics of synaptic BDNF
520 secretion: An update. *Neurosci Res* 65:11–22.
- 521 Lu B, Nagappan G, Lu Y (2014) BDNF and synaptic plasticity, cognitive function, and
522 dysfunction. *Handb Exp Pharmacol* 220:223–250.
- 523 Lund I V, Hu Y, Raol YH, Benham RS, Faris R, Russek SJ, Brooks-Kayal AR (2008) BDNF
524 selectively regulates GABAA receptor transcription by activation of the JAK/STAT pathway.
525 *Sci Signal* 1:ra9.
- 526 McNamara JO, Huang YZ, Leonard AS (2006) Molecular signaling mechanisms underlying
527 epileptogenesis. *Sci STKE* 2006:re12.
- 528 Melchor JP, Strickland S (2005) Tissue plasminogen activator in central nervous system
529 physiology and pathology. *Thromb Haemost* 93:655–660.
- 530 Mowla SJ, Pareek S, Farhadi HF, Petrecca K, Fawcett JP, Seidah NG, Morris SJ, Sossin WS,
531 Murphy RA (1999) Differential sorting of nerve growth factor and brain-derived neurotrophic
532 factor in hippocampal neurons. *J Neurosci* 19:2069–2080.
- 533 Mudò G, Jiang XH, Timmusk T, Bindoni M, Belluardo N (1996) Change in neurotrophins and
534 their receptor mRNAs in the rat forebrain after status epilepticus induced by pilocarpine.
535 *Epilepsia* 37:198–207.
- 536 Müller CJ, Gröticke I, Hoffmann K, Schughart K, Löscher W (2009) Differences in sensitivity to
537 the convulsant pilocarpine in substrains and sublines of C57BL/6 mice. *Genes Brain Behav*
538 8:481–492.
- 539 Nagappan G, Zaitsev E, Senatorov V V, Yang J, Hempstead BL, Lu B (2009) Control of
540 extracellular cleavage of ProBDNF by high frequency neuronal activity. *Proc Natl Acad Sci*
541 *U S A* 106:1267–1272.
- 542 Ng YP, Cheung ZH, Ip NY (2006) STAT3 as a downstream mediator of Trk signaling and
543 functions. *J Biol Chem* 281:15636–15644.
- 544 Pang PT, Teng HK, Zaitsev E, Woo NT, Sakata K, Zhen S, Teng KK, Yung W-H, Hempstead
545 BL, Lu B (2004) Cleavage of proBDNF by tPA/plasmin is essential for long-term
546 hippocampal plasticity. *Science* 306:487–491.
- 547 Reibel S, Larmet Y, Lê BT, Carnahan J, Marescaux C, Depaulis A (2000) Brain-derived
548 neurotrophic factor delays hippocampal kindling in the rat. *Neuroscience* 100:777–788.
- 549 Riffault B, Medina I, Dumon C, Thalman C, Ferrand N, Friedel P, Gaiarsa J-L, Porcher C (2014)
550 Pro-Brain-Derived Neurotrophic Factor Inhibits GABAergic Neurotransmission by Activating
551 Endocytosis and Repression of GABAA Receptors. *J Neurosci* 34:13516–13534.
- 552 Roberts DS, Hu Y, Lund I V, Brooks-Kayal AR, Russek SJ (2006) Brain-derived neurotrophic
553 factor (BDNF)-induced synthesis of early growth response factor 3 (Egr3) controls the
554 levels of type A GABA receptor alpha 4 subunits in hippocampal neurons. *J Biol Chem*
555 281:29431–29435.
- 556 Rudge JS, Mather PE, Pasnikowski EM, Cai N, Corcoran T, Acheson A, Anderson K, Lindsay

- 557 RM, Wiegand SJ (1998) Endogenous BDNF protein is increased in adult rat hippocampus
558 after a kainic acid induced excitotoxic insult but exogenous BDNF is not neuroprotective.
559 *Exp Neurol* 149:398–410.
- 560 Schindelin J, Arganda-Carreras I, Frise E, Kaynig V, Longair M, Pietzsch T, Preibisch S,
561 Rueden C, Saalfeld S, Schmid B, Tinevez J-Y, White DJ, Hartenstein V, Eliceiri K,
562 Tomancak P, Cardona A (2012) Fiji: an open-source platform for biological-image analysis.
563 *Nat Methods* 9:676–682.
- 564 Unsain N, Nuñez N, Anastasía A, Mascó DH (2008) Status epilepticus induces a TrkB to p75
565 neurotrophin receptor switch and increases brain-derived neurotrophic factor interaction
566 with p75 neurotrophin receptor: an initial event in neuronal injury induction. *Neuroscience*
567 154:978–993.
- 568 Volosin M, Trotter C, Cragolini A, Kenchappa RS, Light M, Hempstead BL, Carter BD,
569 Friedman WJ (2008) Induction of proneurotrophins and activation of p75NTR-mediated
570 apoptosis via neurotrophin receptor-interacting factor in hippocampal neurons after
571 seizures. *J Neurosci* 28:9870–9879.
- 572 VonDran MW, LaFrancois J, Padow VA, Friedman WJ, Scharfman HE, Milner TA, Hempstead
573 BL (2014) p75NTR, but not proNGF, is upregulated following status epilepticus in mice.
574 *ASN Neuro* 6.
- 575 Yang J, Harte-Hargrove LC, Siao CJ, Marinic T, Clarke R, Ma Q, Jing D, LaFrancois JJ, Bath
576 KG, Mark W, Ballon D, Lee FS, Scharfman HE, Hempstead BL (2014) ProBDNF
577 Negatively Regulates Neuronal Remodeling, Synaptic Transmission, and Synaptic
578 Plasticity in Hippocampus. *Cell Rep* 7:796–806.
- 579 Yang J, Siao C-J, Nagappan G, Marinic T, Jing D, McGrath K, Chen Z-Y, Mark W, Tessarollo L,
580 Lee FS, Lu B, Hempstead BL (2009) Neuronal release of proBDNF. *Nat Neurosci* 12:113–
581 115.
- 582 Yepes M, Lawrence DA (2004) Neuroserpin: a selective inhibitor of tissue-type plasminogen
583 activator in the central nervous system. *Thromb Haemost* 91:457–464.
- 584

585 **Legends**

586 **Figure 1. Schematic representation of different proteins involved in the cleavage of BDNF**
587 **through extracellular and intracellular mechanisms.** ProBDNF can be cleaved intracellularly
588 within the endoplasmic reticulum by furin and in regulated secretory vesicles by proconvertase
589 enzymes (PC1/3). ProBDNF can also be cleaved extracellularly by matrix metalloproteinases
590 (MMP -3/-7/-9) or by components of the tissue plasminogen activator/plasmin (tPA/plasmin)
591 proteolytic cascade. The activity of these proteases is tightly regulated by a number of inhibitors
592 including plasminogen activator inhibitor 1 (PAI-1) that inhibits both extracellular and
593 intracellular cleavage, tissue inhibitor of metalloproteinases (TIMPs) that inhibit MMPs and

594 neuroserpin and $\alpha 2$ antiplasmin (A2AP) that inhibit the tPA/plasmin proteolytic cascade. Red
595 bars indicate inhibition and green bars indicate activation.

596

597 **Figure 2. ProBDNF protein levels are elevated acutely after pilocarpine induced SE in WT**

598 **C57BL/6J mice.** A) Bottom: Representative western blot of whole hippocampal protein

599 homogenates from WT mice sacrificed 3hr after induction of SE or time-matched saline controls

600 probed with proBDNF (1:1,000) and anti-actin antibodies. Top: densitometry analysis of

601 proBDNF protein abundance. Ratio of proBDNF/Actin at 3hr post-SE (N=5) expressed as

602 percent change relative to mean values (+/- S.E.M.) of control group (N=5; $p < 0.001$). B) Bottom:

603 representative western blot of whole of whole hippocampal protein homogenates from WT mice

604 sacrificed 24hr after induction of SE or time-matched saline controls probed with proBDNF

605 (1:1,000) and anti-actin antibodies. Top: ratio of proBDNF/Actin at 24hr post-SE (N=4)

606 expressed as percent change relative to mean values of control group (N=4; $p < 0.05$).

607

608 **Figure 3. ProBDNF levels are elevated in BDNF-HA tagged mice in the first 24 h after**

609 **pilocarpine induced SE.** A) Top: Representative western blot of whole hippocampal protein

610 homogenates from BDNF-HA mice sacrificed 3hr after induction of SE or time-matched saline

611 controls probed with anti-HA (1:3,000) and anti-actin antibodies. Bottom: Densitometry analysis

612 of proBDNF protein abundance. Ratio of proBDNF/Actin at 3hr post-SE (N=6) expressed as

613 percent change relative to mean values (+/- S.E.M.) of control group (N=3; $p < 0.001$). B) Top:

614 Representative western blot of whole hippocampal protein homogenates from BDNF-HA mice

615 probed with anti-HA (1:3,000) and anti-actin antibodies sacrificed 24hr after induction of SE or

616 time-matched saline controls. Bottom: Densitometry analysis of proBDNF protein abundance at

617 24hr post-SE. Ratio of proBDNF/Actin at 24hr post-SE (N=6) expressed as percent change

618 relative to mean values of control group (N=3; $p < 0.01$). Densitometry analysis of mBDNF

619 protein abundance (mBDNF/Actin) showed no significant difference between control and SE
620 group at either time point.

621

622 **Figure 4. BDNF protein is expressed in neurons and astrocytes of hippocampus after**
623 **pilocarpine induced SE.** A) Representative confocal images of hippocampal subfields from
624 HA-tagged mice 3hr after SE and an age- and handling-matched control (A; 20x magnification,
625 scale bar = 100 μ m) shows presence of HA immunoreactivity in principal cells, glia and mossy
626 fiber layers. The first column shows anti-HA (green) immunoreactivity with DAPI (blue) in each
627 condition. The second column demonstrates co-localization of immunoreactivity for HA (green)
628 and the neuronal marker MAP2 (red). The third column demonstrates co-localization of
629 immunoreactivity for HA (green) and the glial marker GFAP (red). B) High magnification
630 confocal image of CA3 hippocampal subfield (63x magnification, scale bar = 20 μ m). White
631 arrow heads correspond to neuronal localization of HA immunoreactivity in pyramidal cells of
632 CA3; blue arrow heads correspond to localization of HA immunoreactivity in mossy fibers. (SL:
633 stratum lucidum, SP: stratum pyramidale). C) High magnification confocal image of CA3
634 hippocampal subfield (63x magnification, scale bar = 20 μ m) demonstrating glial expression of
635 BDNF.

636

637 **Figure 5. Enzymes involved in the processing of proBDNF are altered after pilocarpine-**
638 **induced SE.** Representative western blots of whole hippocampal protein homogenates from
639 WT mice sacrificed 3hr (left panels) and 24hr (right panels) after induction of SE or time-
640 matched saline controls. Densitometry analysis of abundance of different cleavage proteins
641 normalized to actin and expressed as percent change relative to mean values of control group
642 (+/- S.E.M.). A and B) anti-furin (1:1,000); C and D) anti-plasminogen (1:3,000); E and F) anti-
643 MMP9 (1:2,000); G and H) anti-tPA (1:1,000). The sample size for 3hr is N=5 in each group and
644 for 24hr N=4 in each group (*p<0.05, **p<0.01, ***p<0.001; t-test)

645

646 **Figure 6. Inhibitors of proBDNF processing are altered after pilocarpine SE.**

647 Representative western blots of whole hippocampal protein homogenates from WT mice
648 sacrificed 3hr (left panels) & 24hr (right panels) after induction of SE or time-matched saline
649 controls. Densitometry analysis of abundance of different inhibitor proteins normalized to actin
650 and expressed as percent change relative to mean values of control group (+/- S.E.M.). A and
651 B) anti-alpha2-antiplasmin (A2AP, 1:2,000); C and D) anti-neuroserpin (1:2,000); E and F) anti-
652 TIMP-1 (1:1,000); G and H) anti-PAI-1 (1:1,000). The sample size for 3hr is N=5 in each group
653 and for 24hr is N=4 in each group (**p<0.01, ***p<0.001; t-test).

654

655 **Figure 7. ProBDNF, PAI-1 and tPA levels at 3 and 7 days following SE.** Right:

656 Representative western blots of whole hippocampal protein homogenates from WT mice
657 sacrificed 3 days (top panels) or 7 days (bottom panels) after induction of SE or time-matched
658 saline controls probed with antibodies against proBDNF (A), PAI-1 (B), or tPA (C). Left:
659 Densitometry analysis of abundance of proBDNF (A), PAI-1 (B), or tPA (C) normalized to actin
660 and expressed as percent change relative to mean values of control group (+/- S.E.M.). A) anti-
661 proBDNF (1:2,000); B) anti-PAI-1 (1:1,000); C) anti-tPA (1:1,1000). N=4 for all control groups,
662 and N=8 for all 7 days SE groups. For 3 days SE groups, N=4 for proBDNF and N=5 for PAI-1
663 and tPA (*p<0.05, ***p<0.001; t-test used for all analyses except PAI at 3 days for which Mann
664 Whitney (non-parametric) test was used due to non-normal data set).

665

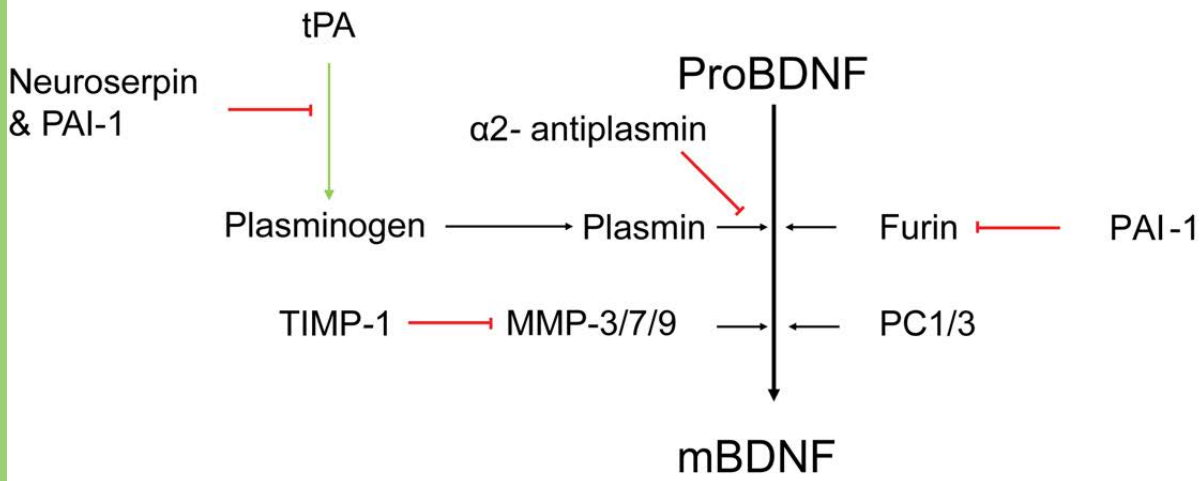
666 **Figure 8. PAI-1 Inhibition reduces proBDNF levels after pilocarpine SE.** Right:

667 representative western blots of protein homogenates from hippocampal slices from individual
668 WT mice removed 24 hours after SE then incubated for four hours in aCSF containing the PAI-1
669 inhibitor tiplaxtinin (370 μ M; TREATED) or vehicle (DMSO; CTRL), probed with anti-proBDNF
670 (1:2,000) or anti-actin antibodies. Left: densitometry analysis of abundance of proBDNF

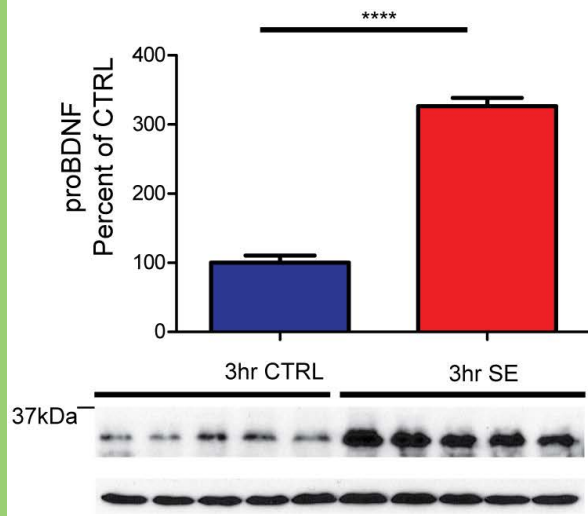
671 normalized to actin in homogenates from vehicle-treated (CTRL) and tiplaxtinin-treated
672 (TREATED) slices for each animal (N=5). Tiplaxtinin treatment resulted in a significant reduction
673 in proBDNF levels compared to vehicle treatment ($p < 0.05$, t-test).

Extracellular Cleavage

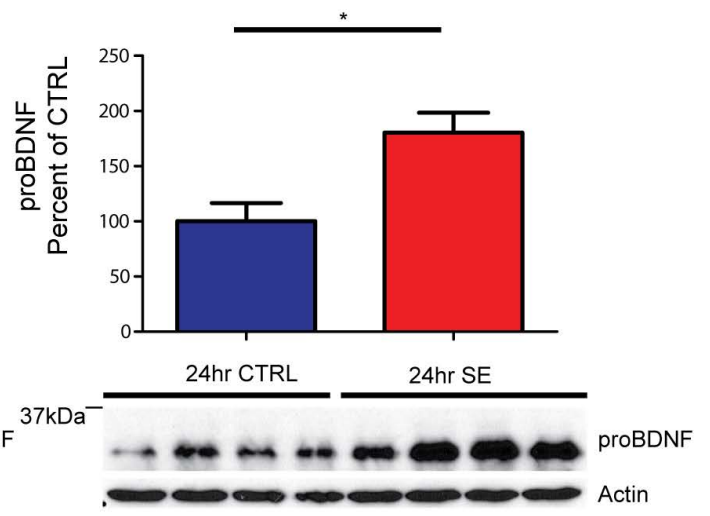
Intracellular Cleavage



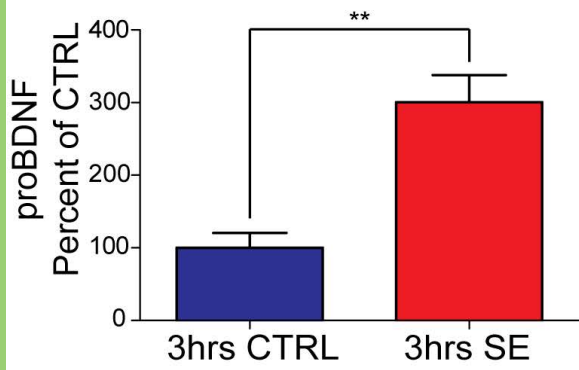
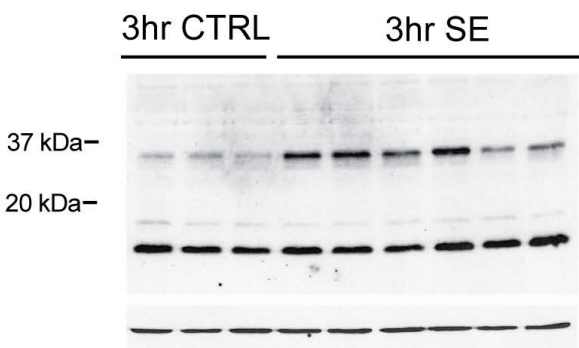
A



B



A



B

